



PAPER • OPEN ACCESS

Effect of Mn addition on magnetoelectric coupling behavior of $\text{BiFeO}_3\text{-Pb/BaTiO}_3$ multiferroics

To cite this article: Naveen Kumar *et al* 2020 *Mater. Res. Express* **7** 015704View the [article online](#) for updates and enhancements.

You may also like

- [Defocus leakage radiation microscopy for single shot surface plasmon measurement](#)
Terry W K Chow, Daniel P K Lun, Suejit Pechprasarn *et al.*
- [Search for Nearby Earth Analogs. I. 15 Planet Candidates Found in PFS Data](#)
Fabo Feng, Jeffrey D. Crane, Sharon Xuesong Wang *et al.*
- [Optimal FPE for non-linear 1d-SDE. I: Additive Gaussian colored noise](#)
Marco Bianucci and Riccardo Mannella

Breath Biopsy Conference

5th & 6th November Online

Join the conference to explore the **latest challenges** and advances in **breath research**, you could even **present your latest work!**

Register now for free!

BREATH BIOPSY

- Main talks
- Early career sessions
- Posters





PAPER

Effect of Mn addition on magnetoelectric coupling behavior of BiFeO₃-Pb/BaTiO₃ multiferroics

OPEN ACCESS

RECEIVED

28 October 2019

REVISED

27 November 2019

ACCEPTED FOR PUBLICATION

10 December 2019

PUBLISHED

6 January 2020

Naveen Kumar¹, Narayan Bastola² , Arun Kumar Singh³ and Sanjeev Kumar¹ ¹ Department of Applied Sciences, Punjab Engineering College (Deemed to be University), Chandigarh, 160012, India² Department of Materials Engineering, Indian Institute of Science, Bengaluru 560012, India³ Electronics and Communications Engineering Department, Punjab Engineering College (Deemed to be University), Chandigarh, 160012, IndiaE-mail: sanjeev04101977@gmail.com**Keywords:** ferroelectric, perovskite, dielectric, morphotropic phase boundary

Original content from this work may be used under the terms of the [Creative Commons Attribution 4.0 licence](https://creativecommons.org/licenses/by/4.0/).

Any further distribution of this work must maintain attribution to the author(s) and the title of the work, journal citation and DOI.

**Abstract**

Hybrid multiferroic materials exhibiting morphotropic phase boundary (MPB) with enhanced ferroelectric and ferromagnetic properties has shown great potential for future technologies. In this paper, we report structural, ferroelectric, piezoelectric, magnetic and magnetoelectric characteristics of 0.7BiFeO₃-0.3Pb_{0.5}Ba_{0.5}TiO₃ (BFPTBT-Pure) and 0.7BiFeO₃-0.3Pb_{0.5}Ba_{0.5}TiO₃ + Mn0.5% (BFPTBT-Mn5%) ceramic compositions synthesized via conventional solid state reaction route. The crystallinity of the compositions exhibits polymorphs of rhombohedral (*R3c*) and tetragonal (*P4mm*) symmetries forming morphotropic phase boundary (MPB). Highly dense SEM micrographs were observed with an average grain size 0.57 μm and 0.62 μm for BFPTBT-Pure and BFPTBT-Mn5%, respectively. Mn doped ceramic sample. Improved ferroelectric behavior has been observed with Mn doping in the composition as the value of remnant polarization increases from 2.46 μC cm⁻² to 7.63 μC cm⁻² recorded at an applied frequency of 50 Hz. The piezoelectric coefficients for BFPTBT-Pure and BFPTBT-Mn5% were found to be 36pC/N and 57pC/N respectively. M-H hysteresis loops depicted that remnant magnetization increases with Mn addition in the sample. The Curie transition temperature (*T_c*) was observed to be 447 °C and 467 °C for BFPTBT-Pure and BFPTBT-Mn5% ceramics, respectively. The magnetoelectric coupling was confirmed through the observation of magnetic field induced relative change in dielectric constant (Magnetocapacitance: *MC*). *MC* was found to be 9.49% and 11.81% for BFPTBT-Pure and BFPTBT-Mn5%, respectively.

1. Introduction

In recent years, an immense interest has been instigated in materials research on ferroelectric systems exhibiting morphotropic phase boundary (MPB) as compositions at and near to MPB attain improved electromechanical properties. The coexistence of two ferroelectric polymorphs is generally referred as MPB. After the discovery of MPB in Pb(Zr_(1-x)Ti_x)O₃ [1] system, it has been found in various other materials such as Pb(Mg_{1/3}Nb_{2/3})O₃-PbTiO₃ and Pb(Mg_{1/3}Nb_{2/3})O₃-PbTiO₃ [2]. Prior to appearance of MPB in multi-ferroelectric systems, first-principle calculations of PbTiO₃ at high pressures realized the formation of MPB region [3] which was later demonstrated experimentally by Ahart *et al* [4]. Recently, co-existing ferroelectric phases have also been observed in strain engineered epitaxial thin films [5, 6]. Therefore, MPB region can be considered and referred as a necessary condition for enhanced electromechanical response in ferroelectric materials. In literature, two important aspects observed related to MPB are (i) Polar vector orientation within the unit cell results in lower symmetry monoclinic phase [7] and (ii) persistence of nanodomain regions [8].

Ferroelectric solid solutions of (1-x)BiFeO₃-xPbTiO₃ have gathered remarkable attention due to several interesting features: (a) High *c/a* ratio, (b) Room temperature polarization with high Curie temperature and (c) Existence of MPB region [9–11]. This material can be considered as a piezoelectric actuator functional up to 500 °C [12]. BiFeO₃ is extensively explored material and exhibits rhombohedrally (space group: *R3c*) distorted

perovskite crystalline phase with unit cell parameters $a = 5.58\text{\AA}$ and $c = 13.9\text{\AA}$ along with $a^- a^- a^-$ octahedral tilting of FeO_6 network [13, 14]. BiFeO_3 possesses high Neel temperature ($T_N \sim 643\text{K}$) and Curie temperature ($T_c \sim 1143\text{K}$) [15]. PbTiO_3 exhibits high Curie temperature ($T_c \sim 763\text{K}$) with tetragonal crystal structure (space group: $P4mm$) and high tetragonal ratio (c/a) ~ 1.06 [16]. It is very difficult to obtain mechanically hard robust ceramic samples of BiFeO_3 - PbTiO_3 ceramic samples due to high tetragonality (c/a) and also due to the existence of negative temperature gradient, which limits the sintering at high temperatures [17, 18]. Different strategies have been imposed to overcome this tribulation via defect chemistry and site engineering. For example, ternary solid solution of BiFeO_3 - PbTiO_3 with PbZrO_3 and BaZrO_3 as an end member showed improved piezo-response [19, 20]. Also BiFeO_3 - PbTiO_3 - BaTiO_3 ternary system exhibits high remnant polarization ($P_r \sim 60 \mu\text{C cm}^{-2}$) and piezoelectric coefficient ($d_{33} = 100\text{pC/N}$) [21].

Szwagierczak and Kulawick reported that electrical resistivity from $10^6\Omega$ to $10^{11}\Omega$ with Mn modification in $\text{Pb}(\text{Fe}_{2/3}\text{W}_{1/3})\text{O}_3$ ceramics [22]. Yao *et al* also observed that Mn addition affects the structural, dielectric and piezoelectric properties of 0.35BiScO_3 - 0.60PbTiO_3 - $0.05\text{Pb}(\text{Zn}_{1/3}\text{Nb}_{2/3})\text{O}_3$ perovskite ceramics [23]. Barranco *et al* studied the effect of Mn modification in PbTiO_3 based perovskite solid solution and found that Mn modification shows high resistivity and improves the ferroelectric properties of the ceramic samples [24]. Zhang *et al* also showed that Mn modification in BiScO_3 - PbTiO_3 solid solutions [25].

Subsequently, in the present work, we have adopted the technique of site-engineering by replacing Pb-site with Ba and also used Mn as an additive to investigate structural, ferroelectric and piezoelectric properties of 0.7BiFeO_3 - $0.3\text{Pb}_{0.5}\text{Ba}_{0.5}\text{TiO}_3$ and 0.7BiFeO_3 - $0.3\text{Pb}_{0.5}\text{Ba}_{0.5}\text{TiO}_3 + \text{Mn}0.5\%$ ceramic compositions. The ceramic samples are prepared via solid state method to get highly dense and insulating ceramic samples with improved electrical properties.

2. Experimental

Multiferroic ceramic compositions of 0.7BiFeO_3 - $0.3\text{Pb}_{0.5}\text{Ba}_{0.5}\text{TiO}_3$ (BFPTBT-Pure) and 0.7BiFeO_3 - $0.3\text{Pb}_{0.5}\text{Ba}_{0.5}\text{TiO}_3 + \text{Mn}0.5\%$ (BFPTBT-Mn5%) were synthesized by conventional mixed oxide reaction method. Initially, high purity analytical grade reagents of Bi_2O_3 , Fe_2O_3 , PbO , TiO_2 , MnO_2 and BaCO_3 were taken as recipe and mixed together in stoichiometric ratio. The powder mixture was pulverized in planetary ball mill (Fritch, pulverisette classic 5 line) for 10–12 h at a speed of 180 rpm in acetone as the mixing agent. The grounded powder mixture was calcined at 820°C for 2h to ensure homogenization and removal of impurities. The resultant calcined mixture was then milled in mortar pestle with 2% PVA (acts as a binding agent) and then compressed in uniaxial solid compressing machine to form 13mm diameter and 1mm thick cylindrical pellets or discs (called as green pellets). The cylindrical discs were covered with alumina crucible and surrounded by powders of same compositions serving the role of spacer for sintering in a muffle furnace at 1020°C for 2h in air. Post sintering, pellets were polished to remove surfacial impurities and one of them was crushed for 30 min to form powder. After crushing, the powders were annealed at 700°C to remove mechanical stresses generated during sintering and milling. Next, the powders were used for crystal phase analysis using x-ray Diffractometer fitted with Nickel -monochromator Rigaku Smartlab (Rigaku, Japan). During the x-ray experiment, Cu K_α line source with nickel filter was used to obtain structural fingerprints of the crushed specimens. As-sintered specimens were used to obtain SEM micrographs (Quanta, ESEM). Thermal etching method has been used to obtain the best micrographs of the specimens. Furthermore, the sintered specimens were silver electroded to proceed further for ferroelectric characterization (Radiant Technologies). Piezoelectric figure of merit d_{33} was figured out using Piezotest PM 300 longitudinal piezoelectric coefficient analyzer. Magnetocapacitance testing has been carried out using self assembled instrument interfaced with LCR meter.

3. Results and discussion

3.1. Structural and microstructural studies

X-Ray diffraction (XRD) pattern of 0.7BiFeO_3 - $0.3\text{Pb}_{0.5}\text{Ba}_{0.5}\text{TiO}_3$ and 0.7BiFeO_3 - $0.3\text{Pb}_{0.5}\text{Ba}_{0.5}\text{TiO}_3 + \text{Mn}0.5\%$ (wt%) ceramic samples sintered at 980°C for 2h are obtained at a scanning rate of $1^\circ/\text{min}$ within scanning angle range of $15^\circ \leq 2\theta \leq 90^\circ$. Pure perovskite phase are observed without any secondary phases $\text{Bi}_2\text{Fe}_4\text{O}_9$ and $\text{Bi}_{24}\text{Fe}_2\text{O}_{39}$ [26] of BiFeO_3 and other traces of pyrochlore. Rietveld refinement method has been employed using FULLProf suit software [27] to determine crystallinity of the samples. As BiFeO_3 exhibits rhombohedral ($R3c$) phase and both BaTiO_3 , PbTiO_3 exhibit tetragonal ($P4mm$) structure; therefore $R3c$ and $P4mm$ model was chosen to fit the profiles. Both the diffraction profiles were well fitted with rhombohedral and tetragonal polymorphs with low value of goodness of fit parameter ($\chi^2 \sim 1.58$ and 1.75) and confirms the existence of morphotropic phase boundary region as usually observed in $(1-x)\text{BiFeO}_3$ - $x\text{PbTiO}_3$ ceramic compositions for $x = 0.3$ [10]. Figure 1 shows the Rietveld refined XRD profiles

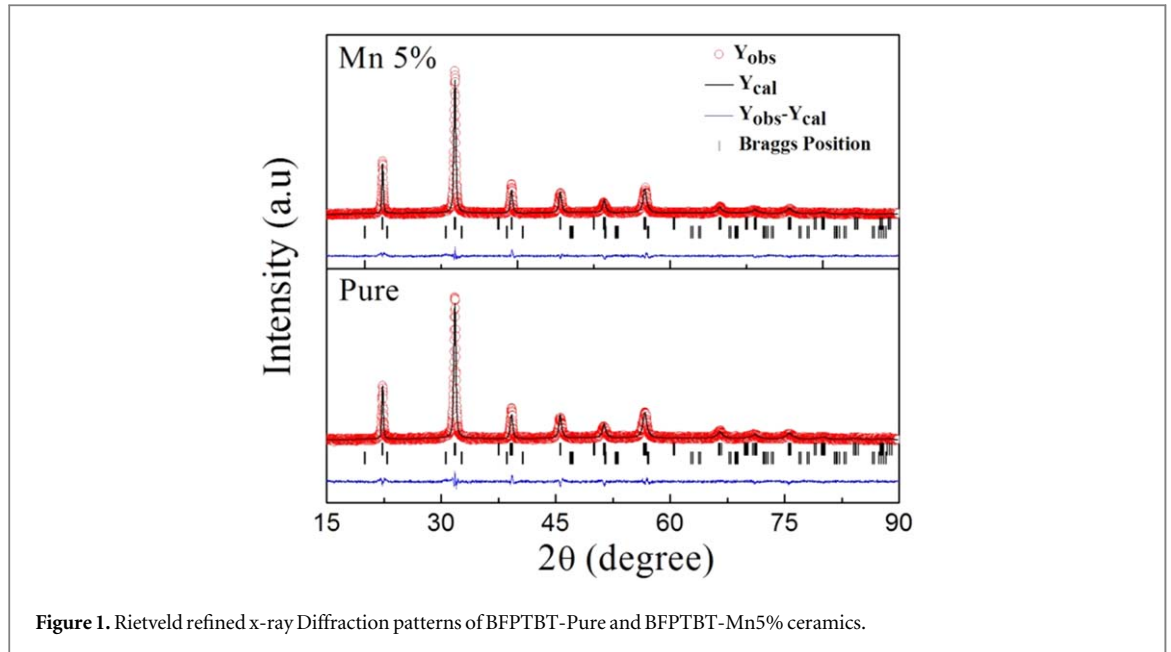


Figure 1. Rietveld refined x-ray Diffraction patterns of BFPTBT-Pure and BFPTBT-Mn5% ceramics.

of both the compositions. The refined statistical factors, lattice parameters, bond angles and bond lengths of the ceramic samples are tabulated in table 1. The stability of perovskite (ABO_3) structure or degree of matching between A and B-site cations can be theoretically calculated by Goldschmidt tolerance factor ' t ' using ionic radii of the elements. The equation for tolerance factor is expressed as given below:

$$t = \frac{[0.7R_{Bi^{3+}} + 0.15R_{Pb^{2+}} + 0.15R_{Ba^{2+}} + R_{O^{2-}}]}{\sqrt{2} [0.7R_{Fe^{3+}} + 0.3R_{Ti^{4+}} + R_{O^{2-}}]} \quad (1)$$

The value of tolerance factor ' t ' calculated using above equation is 0.87.

Figure 2 depicts the surface microstructure of thermally etched specimens of both samples. It can be clearly visualized from the surface micrographs that grains are randomly distributed and inhomogeneous. The average grain size of the particle is calculated using bar diagram as shown in figure 3. The average crystallite size for BFPTBT-Mn5% ($\sim 0.62 \mu\text{m}$) is more than that of BFPTBT-Pure ($\sim 0.57 \mu\text{m}$). It reflects that the grain size slightly increases with intrusion of Mn in the crystal lattice, which thereby acts like an activator and promotes grain growth. Generally, Mn doping helps the sintering performance in Pb-based ceramics significantly [28].

3.2. Ferroelectric studies

Ferroelectric hysteresis loops (P-E loops) of BFPTBT-Pure and BFPTBT-Mn5% ceramic samples measured up to 80 kV cm^{-1} with an applied frequency of 50 Hz are shown in figure 4. Figure 4 clearly depicts that the remnant polarization (P_r) for BFPTBT-Mn5% is more as compared to BFPTBT-Pure sample. The coercive field (E_c) of BFPTBT-Mn5% ceramic sample is also high ($\sim 30 \text{ kV cm}^{-1}$), which signifies stable ferroelectric domain configuration of the ceramic sample. Zheng *et al* [29] has previously reported that Mn^{4+} converts into Mn^{3+} ions with a reaction mechanism as given below:



The ionic radii of Mn^{3+} (64.5pm) is comparable to that of Ti^{4+} (60.5pm) and Fe^{3+} (64.5pm). Therefore, Mn^{3+} ions tend to occupy Fe-site and Ti-site. Mn doping significantly influences the oxygen anion vacancies $V_{O^{2-}}$. Mn^{3+} cations favor occupation at Fe-site and results in an equation:



Mn^{2+} ions capture the anion vacancies and, inhibit the domain wall conduction, thereby resulting enhanced electrical behavior. Also, hybridization between Bi ($6s^2$) lone pair and O ($2p$) orbital of BiFeO_3 crystal and ferroelectric distortion of Ti ($3d$) orbital and O ($2p$) of $(\text{Ba/Pb})\text{TiO}_3$ improves the ferroelectric properties of the specimens.

3.3. Piezoelectric studies

Ceramic samples were poled at 3 kV mm^{-1} at 100°C for 30 min to investigate piezoelectric properties. The piezoelectric coefficient (d_{33}) of BFPTBT-Pure and BFPTBT-Mn5% ceramic compositions were measured using Berlincourt peizo-meter. The value of piezoelectric coefficients is found to be 36 pC/N and 54 pC/N for

Table 1. Statistical parameter, lattice parameter, bond angles and bond lengths of BFPTBT-Pure and BFPTBT-Mn5% ceramics.

Composition	Lattice Parameter (Å)			Cell Volume (Å ³) V	Bond Lengths (R3c)		Bond Angles (R3c)	
	<i>a</i>	<i>b</i>	<i>c</i>		Bi-O	Fe-O	O-Bi-O	O-Fe-O
BFPTBT-Pure Rhombohedral (R- <i>R3c</i>)	5.6149	5.6149	13.8090	377.031	2.651	1.641		
Tetragonal (T- <i>P4mm</i>)	3.8699	3.8699	4.4349	66.418	R: R _{Bragg} = 3.78; R _F = 2.24T: R _{Bragg} = 1.66; R _F = 20.2χ ² = 1.58			
BFPTBT-Mn5% Rhombohedral (R- <i>R3c</i>)	5.6202	5.6202	13.7782	376.900	2.445	1.644		
Tetragonal (T- <i>P4mm</i>)	3.8712	3.8712	4.4326	66.427	R: R _{Bragg} = 3.39; R _F = 1.93T: R _{Bragg} = 1.33; R _F = 17χ ² = 1.75			

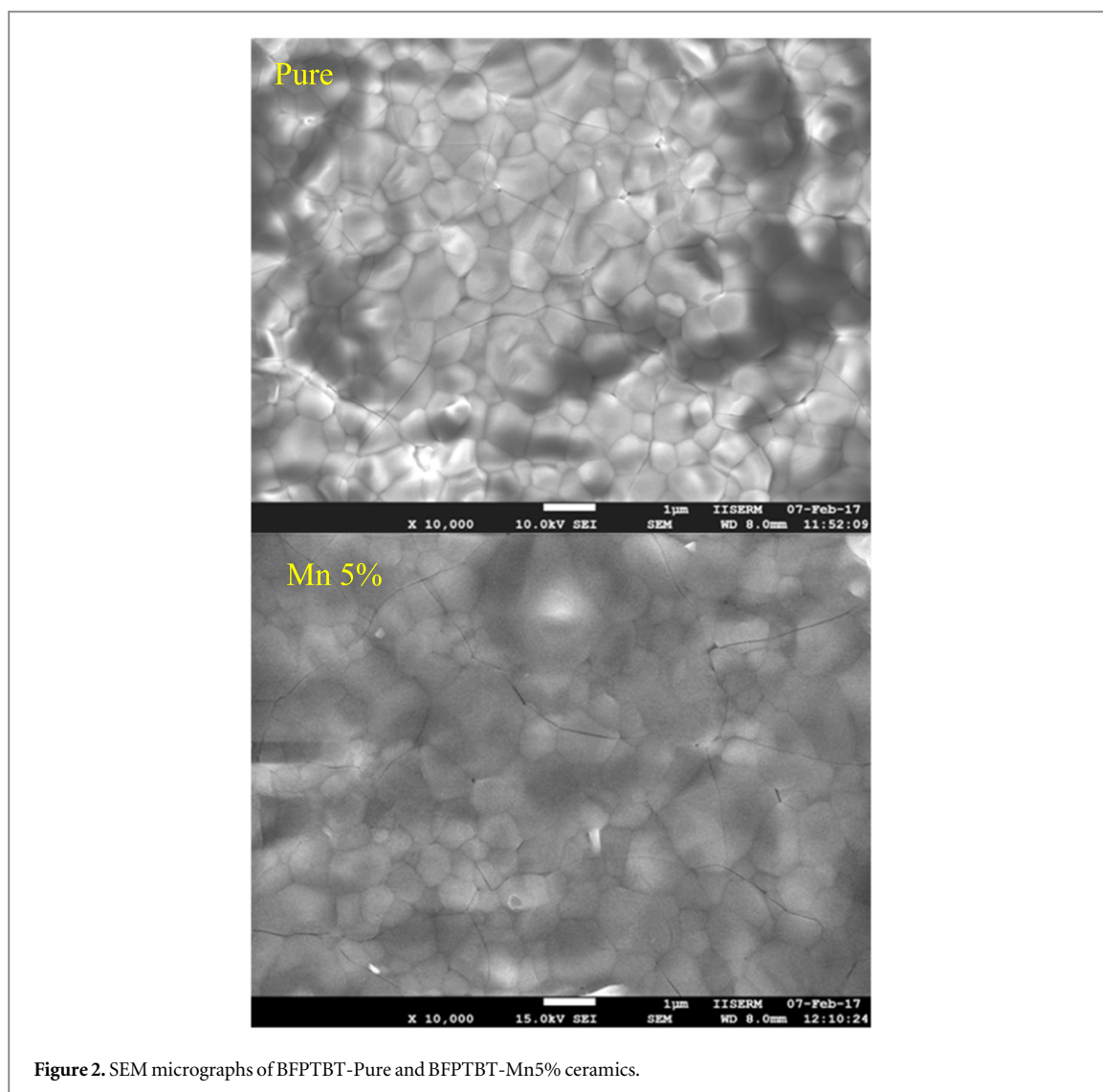


Figure 2. SEM micrographs of BFPTBT-Pure and BFPTBT-Mn5% ceramics.

BFPTBT-Pure and BFPTBT-Mn5%, respectively. It is well observable from the micrographs (as shown in figure 2) that microstructure of BFPTBT-Mn5% sample is highly dense with bigger grain size than that BFPTBT-Pure. Also multiphase coexistence of rhombohedral and tetragonal symmetries being both ferroelectric supports the elevated value of piezoelectric coefficients for both ceramic compositions, which is not observable in $(1-x)\text{BiFeO}_3-x\text{PbTiO}_3$ compositions.

3.4. Magnetic studies

M-H hysteresis loops of BFPTBT-Pure and BFPTBT-Mn5% ceramics sintered at 1020 °C for 2 h are shown in figure 5. It is clearly visualized from the figure 5 that both the ceramic samples exhibit typical ferromagnetic hysteresis loops. Evidently, Mn doping enhances the magnetization and improves greatly the ferromagnetism of the ceramic sample. Zheng *et al* have reported the linear dependence of magnetization on the magnetic field in the case of pure BiFeO_3 as it exhibits G-type antiferromagnetism with long range spin cycloid [30]. But the addition of BaTiO_3 and Mn destroys the space modulated spin cycloid and releases the latent magnetization locked within the spin cycloid. It significantly enhances the magnetization of the $\text{BiFeO}_3\text{-PbTiO}_3$ ceramic composition. The values of remnant magnetization and coercivity for both compositions are given in table 2.

3.5. Dielectric studies

The real part of dielectric constant (ϵ') and tangent loss ($\tan\delta$) as a function of temperature for BFPTBT-Pure and BFPTBT-Mn5% ceramics is shown in figure 6. In the vicinity of the morphotropic phase boundary (MPB) between rhombohedral ($R3c$) and tetragonal ($P4mm$), an anomalous dielectric behavior has been observed for BFPTBT-Pure and BFPTBT-Mn5% compositions [26]. The transition temperature of rhombohedral and tetragonal phases is different as reported by Bhattacharjee *et al* [10]. From the figure 6, it is clearly visualized that two structural transitions exist, one peak is observed near to 200 °C and the other peak is located around 450 °C–

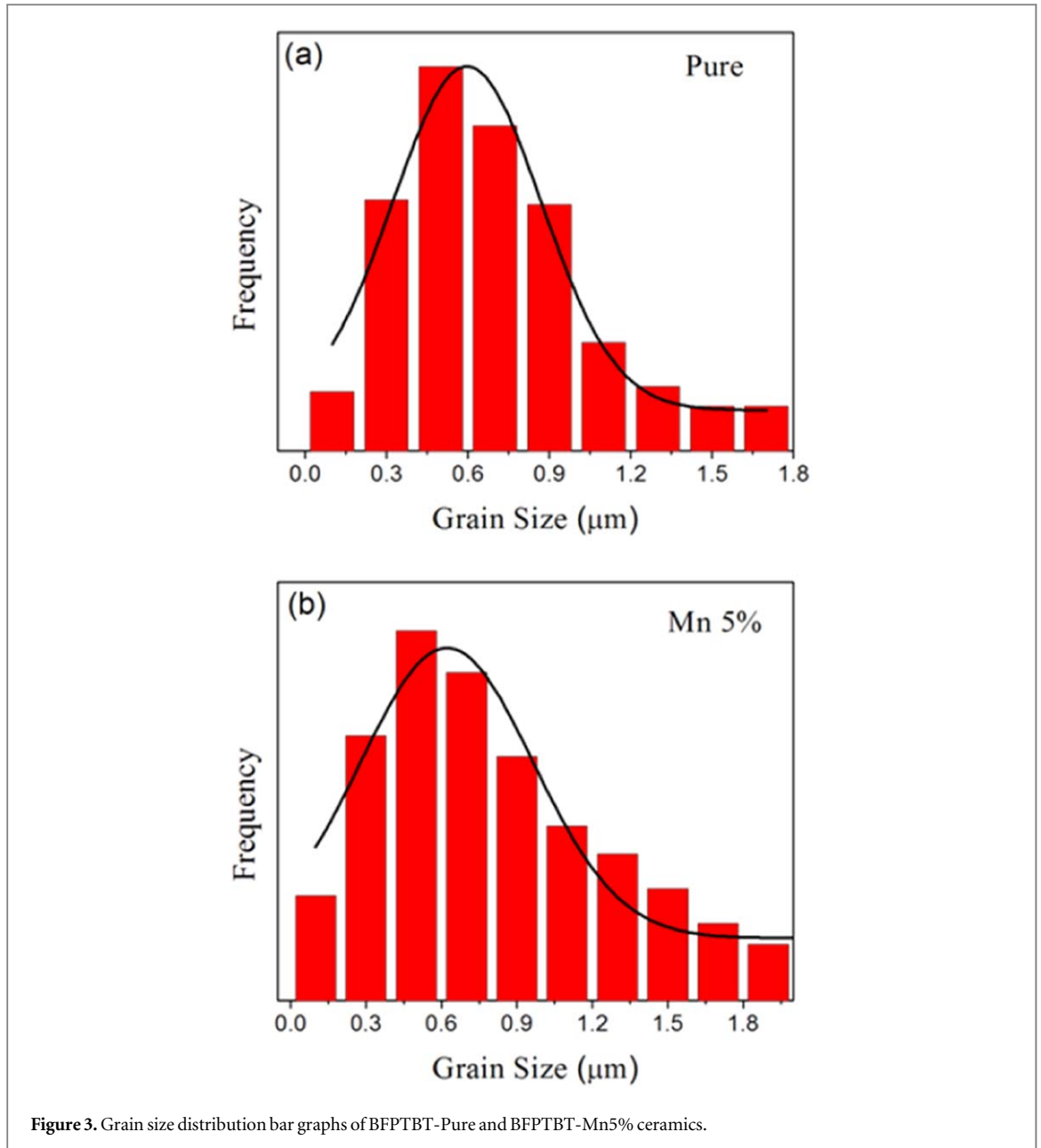


Figure 3. Grain size distribution bar graphs of BFPTBT-Pure and BFPTBT-Mn5% ceramics.

470 °C with low value of dielectric loss for both the compositions. The persistence of dielectric anomalies is consistent with x-ray diffraction studies, where two phase coexistence is confirmed with Rietveld refinement. The enhanced value of remnant polarization for BFPTBT-Mn5% is also a consequence of different progression of phase transition upon heating [31]. The peak value of dielectric permittivity decreases with Mn addition, but the structural transition temperature i.e. Curie temperature (T_c) increases. The value of T_c for BFPTBT-Pure and BFPTBT-Mn5% ceramic composition was found to be 447 °C and 467 °C, respectively.

3.6. Magnetocapacitance analysis

Magnetodielectric or magnetocapacitive effect can be realized by measuring the fractional change in dielectric permittivity as a function of magnetic field. This phenomenon is an alternative and a very simple way to determine magnetoelectric coupling effect of the multiferroic specimen. The magnetocapacitance (MC) can be recorded by using the following expression [32]:

$$MC = \frac{\varepsilon(H) - \varepsilon(0)}{\varepsilon(0)} \times 100 \quad (4)$$

Here, magnetocapacitance is denoted as MC , $\varepsilon(0)$ is the dielectric permittivity measured at zero field and $\varepsilon(H)$ is the dielectric permittivity measured under the influence of applied magnetic field (H). When magnetic field is applied on a multiferroic sample, it experiences strain due to the phenomenon of magnetostriction. The coupling between magnetic and ferroelectric domains also induces stress in the material due to piezomagnetism

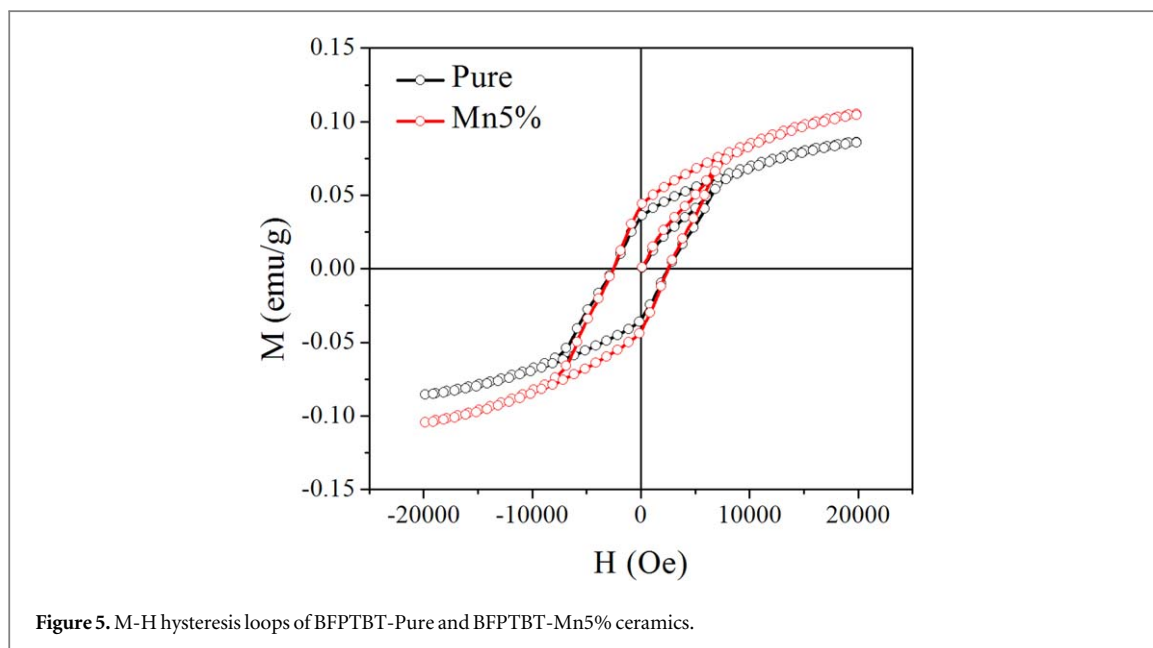
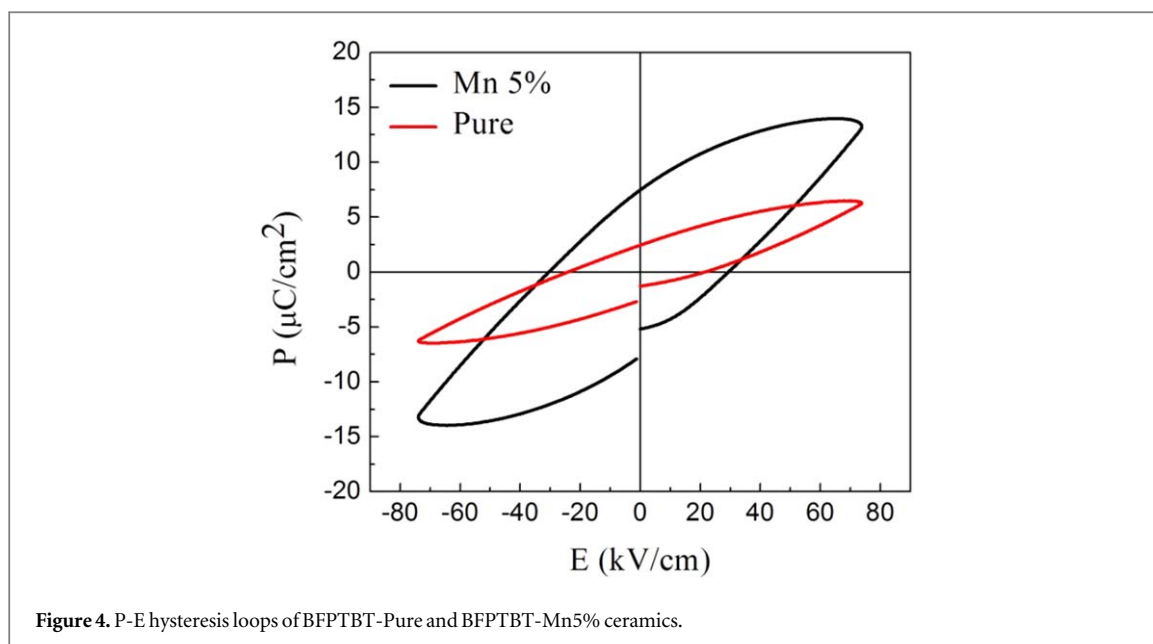


Table 2. Variation of remnant polarization and coercive field of BFPTBT-Pure and BFPTBT-Mn5% ceramics.

Composition	Remnant Polarization (P_r) ($\mu\text{C}/\text{cm}^2$)	Coercive Field (E_c) (kV/cm)	Remnant Magnetization (M_r) (emu/g)	Coercivity (H_c) (Oe)
BFPTBT-Pure	2.46	21.69	0.0350	2514.95
BFPTBT-Mn5%	7.63	30.01	0.0427	2514.95

[33]. Both magnetostriction and piezomagnetism influence the dielectric permittivity of the sample and hence cause substantial variation in dielectric parameters. Furthermore, the existence of dielectric anomaly due to magnetic ordering of ferroelectromagnet could be explained on the basis of Ginzburg–Landau theory of structural phase transition of second order [34]. Smolenski also observed that the appearance of dielectric anomaly in permittivity of the material is mainly due to magnetic ordering of ferroelectromagnet [35]. The relation between thermodynamic potential (φ), electrical polarization (P) and magnetization (M) can be expressed as:

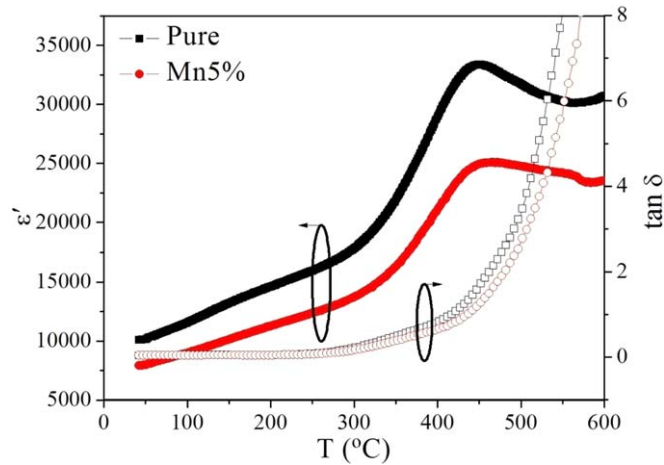


Figure 6. High temperature dielectric permittivity (ϵ') and loss tangent ($\tan\delta$) of BFPTBT-Pure and BFPTBT-Mn5% ceramics at 10 kHz.

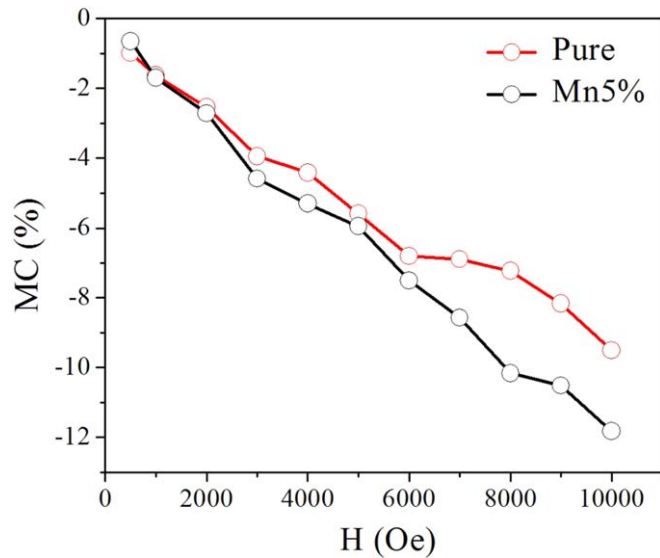


Figure 7. Variation of magnetocapacitance (MC) with magnetic field for BFPTBT-Pure and BFPTBT-Mn5% ceramics.

$$\varphi = \varphi_0 + \alpha P^2 + \frac{\beta}{2} P^4 - PE + \alpha' M^2 + \frac{\beta'}{2} M^4 - MH + \gamma P^2 M^2 \quad (5)$$

Here, α , α' , β , β' and φ_0 are the thermal parameters.

Figure 7 illustrates the fractional variation in dielectric permittivity i.e. magnetocapacitance (MC) as a function of applied magnetic field (H) for BFPTBT-Pure and BFPTBT-Mn5% ceramics. The value of MC was found to be 9.49% and 11.81% for BFPTBT-Pure and BFPTBT-Mn5%, respectively. Table 3 illustrates a comparative of value of MC obtained in the present study with other compounds.

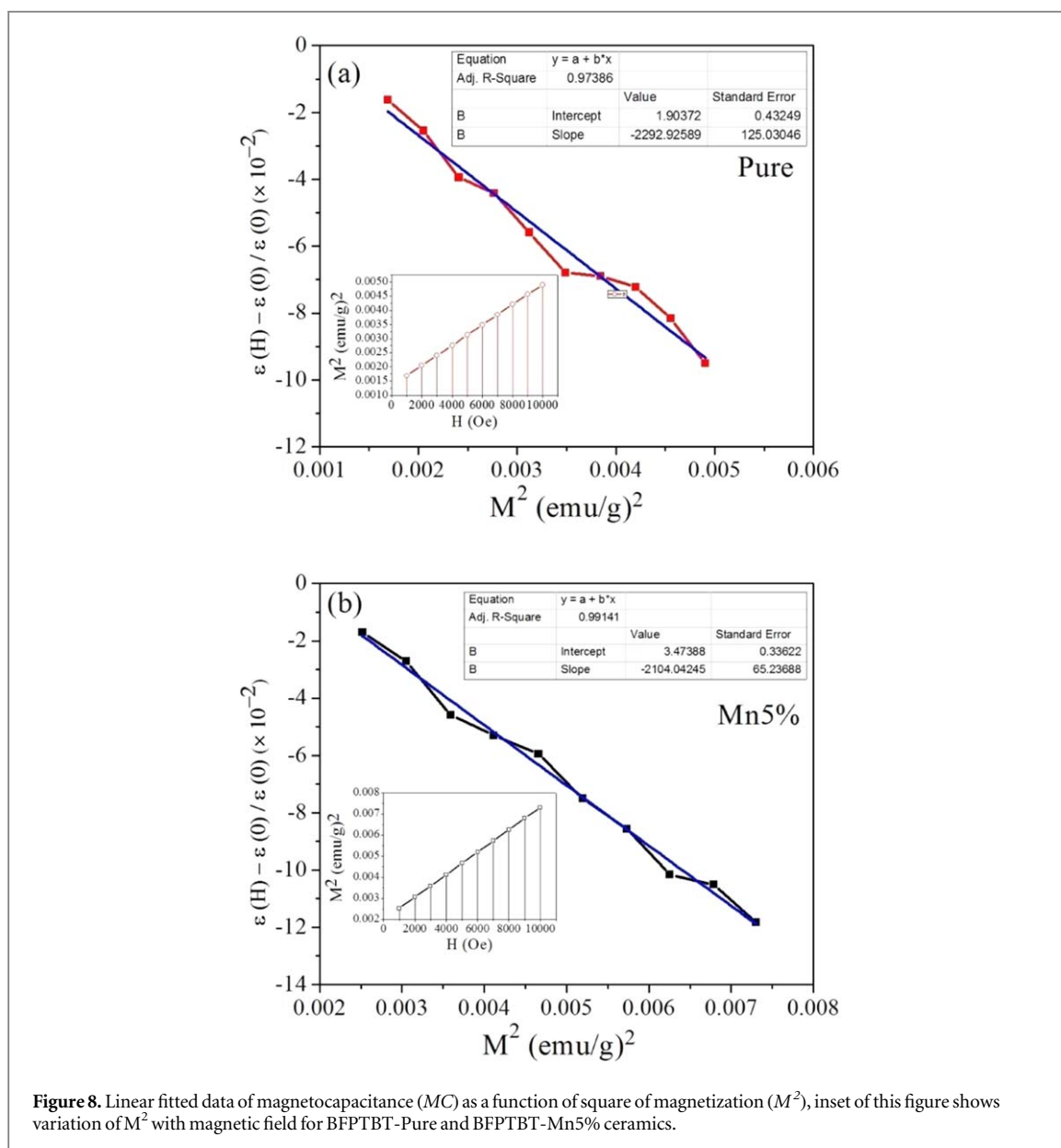
It is reported that MC is directly proportional to square of magnetization (M) [40]:

$$MC \sim \gamma M^2 \quad (6)$$

Here, γ is the magnetic interaction constant. In the present study, the value of magnetic interaction constant is positive for both the compositions. It concludes that the average ferroelectric domains helps in the enhancement of dielectric constant under the influence of applied magnetic field. MC dependence on square of magnetization (M^2) for both compositions is shown in figure 8. The variation in square of magnetization (M^2) as a function of magnetic field up to 10kOe is depicted in the inset of figure 8. These outcomes derive noticeable signature of magnetoelectric coupling in present ceramic compositions.

Table 3. A comparison of the value of magnetocapacitance (MC) with existing reports on multiferroic compounds.

Sr No.	Composition	Magnetocapacitance (MC) (%)	Reference
1	$(\text{BiFeO}_3)_{1-x}-(\text{BaTiO}_3)_x$ at $x = 0.10$	~5	[36]
2	$(1-x)(0.7\text{BiFeO}_3-0.3\text{CoFe}_2\text{O}_4)-x\text{PbTiO}_3$ at $x = 0.45$	2.05	[37]
3	$(1-x)(0.3\text{CoFe}_2\text{O}_4-0.7\text{BiFeO}_3)-x\text{BaTiO}_3$ at $x = 0.40$	3.2	[38]
4	$(1-x)\text{Ba}_{0.70}\text{Ca}_{0.30}\text{TiO}_3-x\text{BiFeO}_3$ at $x = 0.67$	2.96	[39]
5	$0.7\text{BiFeO}_3-0.3\text{Pb}_{0.5}\text{Ba}_{0.5}\text{TiO}_3 + \text{Mn}0.5\%$	11.81%	[Present work]

**Figure 8.** Linear fitted data of magnetocapacitance (MC) as a function of square of magnetization (M^2), inset of this figure shows variation of M^2 with magnetic field for BFPTBT-Pure and BFPTBT-Mn5% ceramics.

4. Conclusions

In this work, we have successfully synthesized pure perovskites BFPTBT-Pure and BFPTBT-Mn5% solid solutions via conventional sintering method. X-Ray diffraction studies revealed the existence of morphotropic phase boundary (MPB) between rhombohedral (R3c) and tetragonal (P4mm) crystalline structures. SEM micrograph illustrates the increment in grain size in BFPTBT-Mn5% ceramic sample as Mn ions dissolves in crystal lattice and promotes the grain growth. Ferroelectric (P-E) hysteresis loops show improved ferroelectric phenomenon in BFPTBT-Mn5% with remnant polarization (P_r) = $7.63 \mu\text{C cm}^{-2}$. In the vicinity of MPB, multiphase coexistence results in enhanced piezoelectric effect as piezoelectric coefficients for 36/N and 57pC/N for BFPTBT-Pure and BFPTBT-Mn5% respectively. M-H hysteresis loops show clear signature of

ferromagnetism for both the compositions and it is observed that remnant magnetization increases with Mn doping. The temperature dielectric studies reveals that high value of Curie temperature i.e. 447 °C and 467 °C is recorded for BFPTBT-Pure and BFPTBT-Mn5%, respectively. Enhanced ferromagnetic contribution led to an overall increase in the magnetocapacitance (MC) for both the compositions. The magnetocapacitance (MC) was increased from 9.49% to 11.81% with Mn doping.

Acknowledgments

Sanjeev Kumar is thankful to DRDO, Govt. of India for financial help in the form of Project ERIP/ER/1604765/M/01/1683. Naveen Kumar is thankful to NRC-M (Materials Engineering, IISc, Bengaluru) for carrying out characterization work.

ORCID iDs

Narayan Bastola  <https://orcid.org/0000-0003-2581-8952>

Arun Kumar Singh  <https://orcid.org/0000-0003-0853-398X>

Sanjeev Kumar  <https://orcid.org/0000-0002-9093-0185>

References

- [1] Jaffe B, Cook W R and Jaffe H 1971 *Piezoelectric Ceramics* (London: Academic)
- [2] Noheda B 2002 *Curr. Opin. Solid State Mater. Sci.* **6** 27
- [3] Rodel J, Jo W, Seifert K T P, Anton E M, Granzow T and Damjanovic D 2009 *J. Am. Ceram. Soc.* **92** 1153
- [4] Wu Z and Cohen R E 2005 *Phys. Rev. Lett.* **95** 037601
- [5] Ahart M, Somayazulu M, Cohen R E, Ganesh P, Dera P, Mao H-k, Hemley R J, Ren Y, Liermann P and Wu Z 2008 *Nature* **451** 545
- [6] Janolin P-E, Bouvier P, Kreisel J, Thomas P A, Kornev I A, Bellaiche L, Crichton W, Hanfland M and Dkhil B 2008 *Phys. Rev. Lett.* **101** 237601
- [7] Fu H and Cohen R E 2000 *Nature* **403** 281
- [8] Jin Y M, Wang Y U, Khachatryan A G, Li J F and Viehland D 2003 *Phys. Rev. Lett.* **91** 197601
- [9] Zhu W-M, Guo H-Y and Ye Z-G 2008 *Phys. Rev. B* **78** 014401
- [10] Bhattacharjee S, Tripathi S and Pandey D 2007 *Appl. Phys. Lett.* **91** 042903
- [11] Ranjan R and Raju A 2010 *Phys. Rev. B* **82** 054119
- [12] Zhu W M and Ye Z-G 2006 *Appl. Phys. Lett.* **89** 232904
- [13] Catalan G and Scott J F 2009 *Adv. Mater.* **21** 2463
- [14] Kubel F and Schmid H 1990 *Acta Crystallogr. B* **46** 698
- [15] Wang Y P, Zhou L, Zhang M F, Chen X Y, Liu J M and Liu Z G 2004 *Appl. Phys. Lett.* **84** 1731
- [16] Siddaramanna A, Srivastava C, Rao B N and Ranjan R 2013 *Solid State Comm.* **160** 56
- [17] Chen J, Xing X R and Liu G R 2006 *Appl. Phys. Lett.* **89** 101914
- [18] Sunder V S, Halliyal A and Umarji A M 1995 *J. Mater. Res.* **10** 1301
- [19] Hu W, Tan X L and Rajan K 2011 *J. Am. Ceram. Soc.* **94** 4358
- [20] Fan L L, Chen J, Li S, Kang H J, Liu L J, Fang L and Xing X R 2013 *Appl. Phys. Lett.* **102** 022905
- [21] Ning H, Lin Y, Hou X and Zhang L 2014 *J. Mater. Sci., Mater. Electron.* **25** 1162
- [22] Szwagierczak D and Kulawik J 2005 *J. Eur. Ceram. Soc.* **25** 1657
- [23] Yao Z, Liu H, Cao M, Hao H and Yu Z 2011 *Mater. Res. Bull.* **46** 1257
- [24] Barranco A P, Pinar F C, Martinez P and Garcia E T 2001 *J. Eur. Ceram. Soc.* **21** 523
- [25] Zhang S J, Eitel R E, Randall C A, Shrout T R and Alberta E F 2005 *Appl. Phys. Lett.* **86** 262904
- [26] Xu J M, Wang G M, Wang H X, Ding D F and He Y 2009 *Mater. Lett.* **63** 855
- [27] Carvajal R J 2008 *FullPROF A Rietveld Refinement and Pattern Matching Analysis Program Laboratories Leon Brillouin (France: [CEA-CNRS])*
- [28] Yao Z, Liu H, Cao M, Hao H and Yu Z 2011 *Mater. Res. Bull.* **46** 1257
- [29] Zheng Q, Luo L, Lam K H et al 2014 *J. Appl. Phys.* **116** 184101
- [30] Amorin H et al 2014 *J. Appl. Phys.* **115** 104104
- [31] Jethva S et al 2017 *Ferroelectrics* **516** 106–16
- [32] Kumar A and Yadav K L 2011 *Matr. Sci. and Engg. B* **176** 227–30
- [33] Shah J and Kotnala R K 2012 *Scrip. Mater.* **67** 316–9
- [34] Kimur T, Kawamoto S, Yamada I, Azuma M, Takano M and Tokura Y 2003 *Phys. Rev. B* **67** 180401
- [35] Smolenskii G A 1962 *Fiz. Tverd. Tela (Leningrad)* **4** 1095 [Sov. Phys. Solid State 4, (1962) 807.]
- [36] Shariq M, Kaur D, Chandel V S and Siddiqui M A 2015 *Acta Phy. Polo. A* **127** 1675–9
- [37] Adhlakha N, Yadav K L and Singh R 2015 *J. Mat. Sci.* **50** 2073–84
- [38] Adhlakha N, Yadav K L and Singh R 2014 *Smart Mater. Struct.* **23** 105024
- [39] Li C X, Yang B, Zhang S T, Zhang R, Sun Y, Zhang H J and Cao W W 2014 *J. Am. Ceram. Soc.* **97** 816–25
- [40] Kumar A and Yadav K L 2011 *J. Phys. Chem. Sol.*, **72** 1189–94